

Investigating the Effects of Brownian Movement and Soret Effect on Convection in Magnetohydrodynamic Jeffrey Fluid Flow

Masarath Jabeen¹, V Dhanalaxmi^{2*}

^{1,2}University college of Science, Osmania University, Hyderabad

Abstract:- This research examined how Brownian motion and Soret effect influenced convection in MHD Jeffrey stream above a horizontal porous plane, with a magnetic field present. The fluid moved above the plate at $y > 0$, with the plate extending infinitely in the x -direction and the flux B_0 applied vertically along the ordinate. Using similarity transformation, the governing coupled nonlinear rapidness, temperature, and concentration boundary layer equations were transmuted into interconnected nonlinear ODEs. The resulting 4th order and 2nd order differential equations were then transmuted into 1st order ODEs using the shooting method. These equations were numerically computed utilizing the `bvp4c` function in MATLAB. The effects of porosity and wall transpiration on the velocity and the effect of various parameters were studied using graphs.

Keywords: MHD Jeffery fluid, Brownian movement, Soret effect porous plate.

1. Introduction

The Jeffrey fluid stands out as a remarkable example of non-Newtonian fluids. Among the several non-Newtonian fluid representations, the Jeffrey fluid flow representation is particularly significant, offering a comprehensive and precise description of viscoelastic fluid properties. Magnetohydrodynamics (MHD) examines the behavior of electrically conductive fluids in motion when subjected to magnetic fields. Some of its uses include plasma confinement, cooling nuclear reactors with liquid metal, utilizing electromagnetic techniques for metal casting, and magnetohydrodynamic (MHD) systems for electricity generation, and geothermal energy extraction [4] Choi & Eastman, 1995; [5] Cramer and Pai, 1973. Knowledge of the convection in MHD flows is essential in these application areas for the design and improvement of such systems, and it is also a non-Newtonian fluid that has viscoelastic property. It can properly simulate different industrial fluids such as polymers, paints, oils, and liquid crystals because they violate Newtonian physics [7] Hayat and Mustafa (2010). Jeffrey's fluid model has included the effect of the proportion between relaxation and retardation durations which makes it closer to real-life fluid flows than other basic viscoelastic models.

Research on MHD flow and heat/mass shift over permeable plane is essential in filtration technology, thermal insulation engineering, oil recovery, and packed bed reactors. The transpiration effect, modelling injection/suction of fluid through the boundary, is useful in cooling metallic plates, chemical processing equipment, membrane filtration processes, and boundary layer control [3] Agarwal & Ahmad, 2017. The existence of a magnetic field is a positive factor and a negative factor because it contributes to the complications and functionality of these industrial uses.

While there is a vast literature on heat transfer characteristics of viscous/Newtonian fluids under various configurations, studies relating to non-Newtonian fluids are scarce [1] Abel et al., 2009; [2] Abel and Mahesha, 2008; [8] Hayat et al., 2010. A literature review reveals that there are very few publications on MHD Jeffrey fluid flows with heat and mass transfer effects, especially involving wall transpiration and porous media, which are mathematically complex.

Thermal energy transfer in MHD viscoelastic fluid flow along a plane analyzed analytically and numerically by Abel et al. [25] 2002 analytically and numerically. However, their work was restricted to viscoelastic fluids, without the inclusion of the Jeffrey fluid model. Noor et al.[10] 2014, in their research

carried out in 2011 analyzed the hydromagnetic movement of Jeffrey fluid across a extended surface in the framework of nanoparticle mass transfer. However, "The effects of thermal radiation was not incorporated into the model. Subsequently, Nadeem et al. [11] 2012, Investigated the laminar boundary layer stagnation-point discharge of a Jeffrey fluid on an extending surface. The researchers examined how Brownian movement and soot effect affected the convection coefficients of the nanoparticles. However, the flow configuration was less complex, and the influence of the magnetic fields was eliminated. Recently, Abd-Alla et al.[12] 2022 discussed The wavelike movement of a Jeffrey fluid through an uneven passage, considering convection consequences. When the thermal radiation response was incorporated, the magnetic field and wall transpiration effects were not considered. Subsequently, Hayat et al.[9] (2015) incorporated thermal radiation and heat source/sink effects into analyzing a transient MHD rotating Jeffrey fluid flow over a stretching sheet. However, this analysis also excluded mass transfer and medium porosity factors. The intricate interplay between heat and mass transfer involving nanoparticles when considering the MHD radiative-convective Movement of Jeffrey fluid across a porous surface with wall transpiration does not appear to have been studied earlier, and this is the reason for the present work. Srikanth G V P N et al.[13] (2014) studied Magnetohydrodynamic nanofluid with chemical reaction effects: An examination of convection, by Achala. L. N and Sathyanarayana. S. B[14] 2011 investigated "Fluid over nonlinearly stretching sheet with magnetic field by homotopy analysis method," Journal of Applied Mathematics and Fluid Mechanics. Krishnendu Bhattacharyya [15] 2013 gave intensified study on "Boundary layer stagnation-point flow of Casson fluid and heat transfer towards a stretching/shrinking sheet", Advances in heat and mass transfer. M. Qasim [16] 2013 "Heat and mass transfer in a Jeffrey fluid over a stretching sheet with heat source/sink". Masarath Jabeen*, V Dhanalaxmi,[17-19] investigated on Numerical investigation of heat and mass transfer in a Jeffrey Fluid flowing over a sheet with linear stretching and chemical reactions: A study examining the combined influence of viscous dissipation and Ohmic heating on magnetohydrodynamic Jeffrey nanofluid flow incorporating magnetic dipole effects. Mohammed. J. Uddin et al. [20] 2012 "MHD free convective boundary layer flow of a nanofluid past a flat vertical plate with Newtonian heating boundary condition." Jakati et al. [21] To study the effects Scientists employed the Jeffrey fluid model to examine Brownian movement and soot effect on nanofluid extending. In a complementary investigation, Ghafouri et al.[22] 2017 analyzed how different thermal conductivity models affected combined convection heat transfer in a square enclosure containing water-alumina nanofluid. The objectives of the present work are to establish a theoretical and computational analysis of heat and nanoparticle mass transfer in the MHD radiative flow of a Jeffrey viscoelastic fluid over a horizontal porous plate with suction injection. These are performed for a steady, laminar, two-dimensional, boundary layer flow configuration. The thermal radiation heat transfer, temperature-dependent heat generation, and absorption were considered. The buoyancy forces were excluded from the flow model. The fundamental partial differential equations representing momentum conservation, heat transfer, and nanoparticle distribution were converted into a more suitable format. These transformed A precise finite-difference-based shooting technique is utilized for the numerical resolution of ODEs. The effects of newly introduced dimensionless control variables on the rapidity, temperature, and concentration outline within the boundary layer are thoroughly examined through comprehensive visual representations and analysis. Therefore, the present study offers a theoretical analysis and is supported by numerical simulation to elaborate the multifaceted transport characteristics of radiative hydromagnetic boundary layer flows of Jeffrey fluid with transpiration boundary conditions and buoyancy forces excluded.

2. Mathematical formulations

The core equations that characterize Jeffrey fluid can be represented as

$$\tau = -pl + E \quad (1)$$

$$E = \frac{\mu}{1+\lambda_1} \left[R_1 + \lambda_2 \left(\frac{\partial R_1}{\partial t} + V \cdot \Delta \right) R_1 \right] \quad (2)$$

In this equation, E represents the additional stress tensor, τ denotes the Cauchy stress tensor, λ_1 and λ_2 are the Jeffrey fluid's material parameters, and R_1 signifies the Rilin-Ericksen tensor, which is defined by the given expression.

$$R_1 = (\nabla V) + (\nabla V)'$$

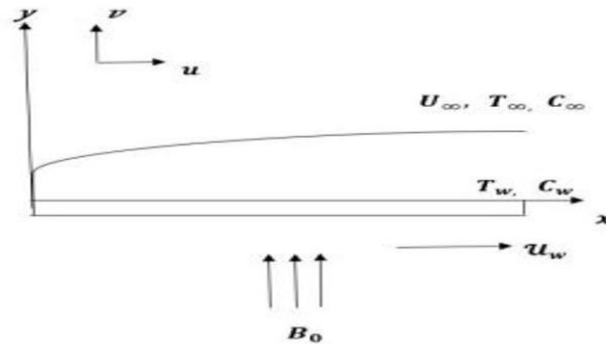


Fig. 1. Physical model of problem

This study investigates the behavior of a steady two-dimensional incompressible, conductive Jeffrey fluid as it moves over a linear extended sheet. The investigation considers the consequences of chemical reactions, thermal radiation, and heat sources on the fluid flow. The sheet's linear stretching is induced by the employment of equal and opposite forces along the x-axis, which generates the fluid motion. Perpendicular to the sheet is the y-axis, with the origin fixed as shown in fig 1.

The power index m characterizes how both temperature and species concentration change in relation to the distance from the origin. The rapidity at which the sheet is extended varies. $U_w(x)$ at $t = 0$.

Under these assumptions, the governing equation of continuity and momentum takes the following form

$$\frac{\partial u}{\partial x} + \frac{\partial v}{\partial y} = 0 \quad (3)$$

$$u \frac{\partial u}{\partial x} + v \frac{\partial u}{\partial y} = \frac{v}{1+\lambda_1} \left[\frac{\partial^2 u}{\partial y^2} + \lambda_2 \left(u \frac{\partial^3 u}{\partial x \partial y^2} + v \frac{\partial^3 u}{\partial y^3} - \frac{\partial u}{\partial x} \frac{\partial^2 u}{\partial y^2} + \frac{\partial u}{\partial y} \frac{\partial^2 u}{\partial x \partial y} \right) \right] + \frac{\mu_0}{\rho} M \frac{\partial H}{\partial x} \quad (4)$$

In this context, u, v represent the rapidity components along the x and y axes, respectively. The momentum diffusivity is denoted by ν while λ_1 signifies the ratio between relaxation and retardation time. Additionally, λ_2 indicates the relaxation time. A dipole field exerts influence on the flow of magnetic fluid, and the scalar potential of the permanent magnet is represented by ϕ .

$$\phi = \frac{\gamma}{2\pi} \left(\frac{x}{x^2 + (y+a)^2} \right)$$

The resultant magnitude of H of the magnetic field intensity is given by

$$H = \sqrt{\left[\left(\frac{\partial \phi}{\partial x} \right)^2 + \left(\frac{\partial \phi}{\partial y} \right)^2 \right]}$$

$$\frac{\partial H}{\partial x} = -\frac{\gamma}{2\pi} \left(\frac{2x}{(y+a)^4} \right)$$

$$\frac{\partial H}{\partial y} = -\frac{\gamma}{2\pi} \left(\frac{-2}{(y+a)^3} + \frac{4x^2}{(y+a)^5} \right)$$

Temperature can be used to express magnetization $M = K^*(T_c - T)$ as a linear relationship.

with the K^* paramagnetic coefficient represented by the Curie temperature denoted as T_c . However, it is crucial to note that this relationship is fundamental for manifesting ferrohydrodynamic interaction.

The equation of heat transfer is given as

$$\rho c_p \left(u \frac{\partial T}{\partial x} + v \frac{\partial T}{\partial y} \right) = k \left(\frac{\partial^2 T}{\partial x^2} + \frac{\partial^2 T}{\partial y^2} \right) + \frac{(\rho c)_p}{(\rho c)_f} (D_B \frac{\partial c}{\partial x} \frac{\partial T}{\partial x} + \frac{\partial c}{\partial y} \frac{\partial T}{\partial y} + \frac{D_T}{T_\infty} \left[\left(\frac{\partial T}{\partial x} \right)^2 + \left(\frac{\partial T}{\partial y} \right)^2 \right]) \quad (5)$$

In this context, c_p represents the massic heat capacity, while k denotes the diffusivity, T indicates the fluid's temperature, and T_∞ signifies the fluid's constant temperature at a considerable distance from the sheet. The nanoparticle volume fraction is represented by C , with D_B and D_T referring to the Brownian diffusion coefficient and thermophoretic diffusion coefficient, respectively. $(\rho c)_p$ symbolizes the effective heat capacity of nanoparticles, and $(\rho c)_f$ represents the heat capacity of the base fluid.

A technique for calculating the flux of radiative heat q_r is offered by the Rosseland diffusion approximation.

$$q_r = -\frac{4\sigma^* \partial T^4}{3K_s \partial y} \quad (6)$$

The Rosseland mean absorption coefficient K_s is represented by this equation, with symbolizing the Stefan-Boltzmann constant σ^* . Given that the temperature T^4 , within the fluid flow is considered to be comparatively low, it can be expressed as a linear function of temperature.

$$T^4 \approx 4T_\infty^3 T - 3T_\infty^4 \quad (7)$$

On solving (6) (7) and (5) we get

$$\frac{\partial q_r}{\partial y} = -\frac{16\sigma^* T_\infty^3}{3K_s} \frac{\partial^2 T}{\partial y^2}. \quad (8)$$

A dimensionless temperature variable $\theta(\zeta)$ is presented, which takes the form:

$$\theta(\zeta) = \frac{T - T_\infty}{T_w - T_\infty} \quad (9)$$

The laminar boundary layer flow's first-order chemical reaction, incorporating concentration diffusion, is expressed as

$$u \frac{\partial C}{\partial x} + v \frac{\partial C}{\partial y} = D \left(\frac{\partial^2 C}{\partial x^2} + \frac{\partial^2 C}{\partial y^2} \right) + \frac{D_T}{T_\infty} \left(\frac{\partial^2 T}{\partial x^2} + \frac{\partial^2 T}{\partial y^2} \right). \quad (10)$$

In this context, D represents the coefficient of diffusion.

We present a temperature variable without dimensions, denoted as $\phi(\zeta)$, which takes the following form:

$$\phi(\zeta) = \frac{C - C_\infty}{C_w - C_\infty} \quad (11)$$

3. Boundary Conditions

To incorporate the effect of boundary surface stretching that induces flow in the x -direction, the following boundary conditions for velocity, temperature, and concentration are considered appropriate:

$$u = U_w(x) = cx, v = 0 \text{ at } y = 0$$

$$u \rightarrow 0, u' \rightarrow 0 \text{ as } y \rightarrow \infty$$

$$T = T_w = T_\infty + A_1 \left(\frac{x}{l} \right)^m \text{ at } y=0$$

$$T \rightarrow T_\infty \text{ as } y \rightarrow \infty$$

$$C = C_w = C_\infty + A_2 \left(\frac{x}{l} \right)^m \text{ at } y=0$$

$$C \rightarrow C_\infty \text{ as } y \rightarrow \infty \quad (12)$$

In this context, constants are represented by A_1, A_2 and l , while l denotes the characteristic length. The surface temperature parameter is symbolized by m , and T_w signifies the stretching sheet temperature. Additionally, C_w and C_∞ indicate the levels of concentration at the surface and at a significant distance away from the surface, respectively. To resolve equations (4), (5), and (10), the following similarity transformations are employed.

$$u = cx f'(\xi), v = -\sqrt{cv} f(\xi) \text{ where } \xi = \sqrt{\frac{c}{v}} y \quad (13)$$

Where ξ is the correspondence variable and $f(\xi)$ is the nondimensional stream function

Substituting eq (13) in eq (4) (5) and (10) we obtain second and fourth order ODEs as follows

$$f'''' + (1 + \lambda_1)(f f'' - f'^2) + \beta(f''^2 - f f^{iv}) - (1 + \lambda_2) \frac{2\beta\theta_1}{(\eta + \alpha_1)^4} = 0 \quad (14)$$

$$\theta'' + Pr(f\theta' + N_b\phi'\theta' + N_t\theta'^2) = 0 \quad (15)$$

$$\phi'' + LePr(f\phi') + \frac{N_t}{N_b}\theta'' = 0 \quad (16)$$

With boundary conditions (12), takes the following form.

$$f(\xi) = s, f'(\xi) = 1 \text{ at } \xi = 0; f'(\xi) = 0, f''(\xi) = 0 \text{ as } \xi \rightarrow \infty$$

$$\theta(\xi) = 1 \text{ at } \xi = 0; \theta(\xi) = 0 \text{ as } \xi \rightarrow \infty$$

$$\phi(\xi) = 1 \text{ at } \xi = 0; \phi(\xi) = 0 \text{ as } \xi \rightarrow \infty$$

In this context, $\beta = \lambda_2 c$ represents the Deborah number, $R = \frac{4\sigma^* T_\infty^3}{K_s}$ signifies the radiation parameter, $Pr = \frac{\rho c_p}{k}$ denotes the Prandtl number, $\gamma = \frac{Qv}{\rho c_p}$ indicates a heat source parameter, $Sc = \frac{v}{D}$ stands for the Schmidt number, $Kr = \frac{Kr^* \delta^2}{v}$ represents the chemical reaction factor, and $s = \frac{-v_w}{\sqrt{cv}}$ is a parameter where $s > 0$.

The non-linear ordinary differential equations (14), (15), and (16), along with their associated boundary conditions (17), are transformed into ODEs utilizing the shooting technique. The numerical solution is then obtained through MATLAB's bvp4c function. This process reduces the 4th order and 2nd order equations to a set of 1st order simultaneous equations.

$$f = y(1), f' = y(2), f'' = y(3), f''' = y(4)$$

$$\theta = y(5), \theta' = y(6)$$

$$\phi = y(7), \phi' = y(8) \quad (18)$$

Substituting these in (14)(15)(16) and (17) we have

$$y(4) + (1 + \lambda)(y(1)y(3) - y(2)^2) + \beta(y(3)^2 - y(1)y(4)') = 0 \quad (19)$$

$$y'(6) + Pr[y(1)y(6) + N_b y(8)y(6) + N_t y(6)] = 0 \quad (20)$$

$$y'(8) + LePr[y(1)y(8) + \frac{N_t}{N_b} y'(6)] = 0 \quad (21)$$

With boundary conditions

$$y_0(1) = 1, y_0(2) = 1; y_\infty(2) = 0, y_\infty(3) = 0; y_0(5) = 1, y_\infty(5) = 0; y_0(7) = 1, y_\infty(7) = 0; y_0(8) = 1, y_\infty(8) = 0$$

The system of equations represented by (19), (20), and (21) is simplified into eight concurrent first-order equations.

$$y'(1) = y(2)$$

$$y'(2) = y(3)$$

$$y'(3) = y(4)$$

$$y'(4) = (y(4) - (1 + \lambda_1)(y(2)^2 - y(1)y(3)) + \beta y(3)^2 + (1 + \lambda_1)((2\gamma_1\vartheta_1)/(\eta + \alpha_1)^4)/(\beta y(1)) \quad (22)$$

$$y'(5) = y(6)$$

$$y'(6) = -Pr[y(1)y(6) + N_b y(8)y(6) + N_t y(6) = 0 \quad (23)$$

$$y'(7) = y(8)$$

$$y'(8) = -LePr[y(1)y(8) + \frac{N_t}{N_b}y'(6) \quad (24)$$

The governing equations are solved numerically using MATLAB's bvp4c function.

4. Result and Discussion

Figures 2 and 3 demonstrate that the fluid's concentration rises as the Prandtl number increases.

Figure 4 illustrates that the fluid's temperature decreases with rise in the N_t parameter. Figure 5 indicates that the fluid's concentration grows as N_b increases.

Figure 6 reveals that the fluid's radial velocity diminishes with rise in the λ_1 parameter.

Figures 7 and 8 depict the changes in the fluid's temperature and concentration in relation to the λ_1 parameter. Lastly,

Figure 9 displays how the fluid's velocity varies with respect to the λ_1 parameter.

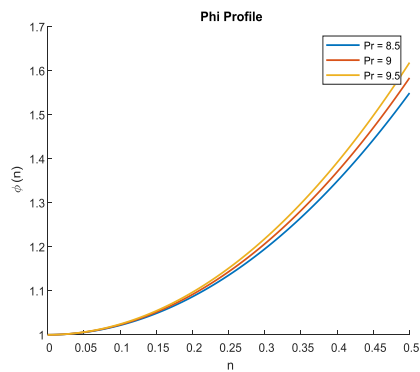


Fig. 2.

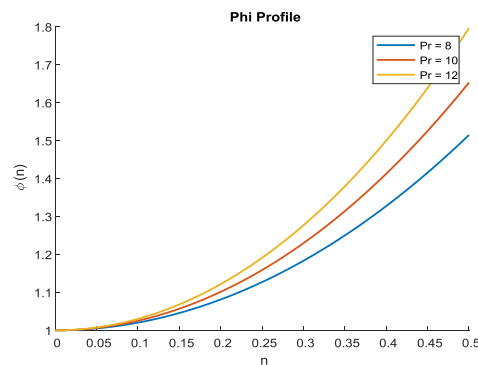


Fig. 3.

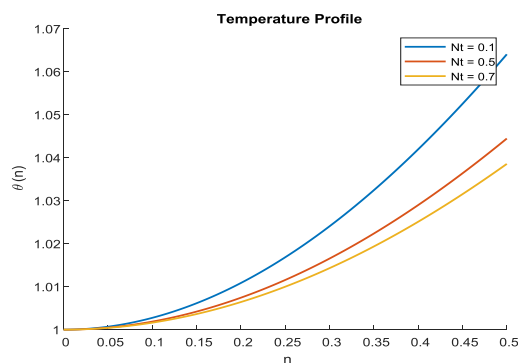


Fig. 4.

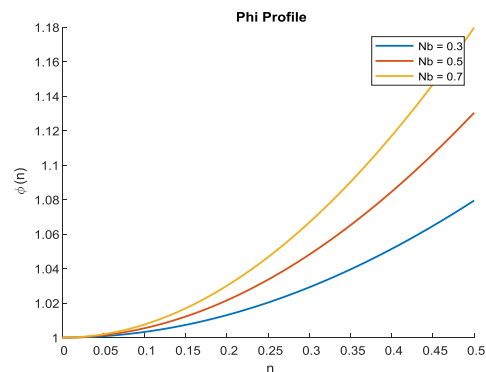


Fig. 5.

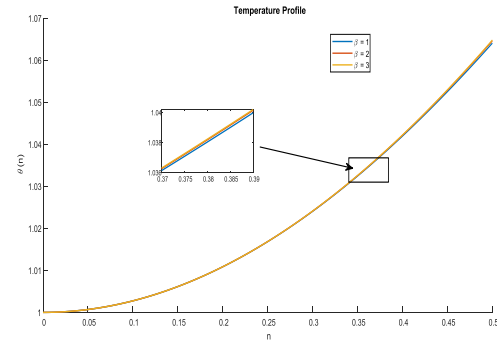
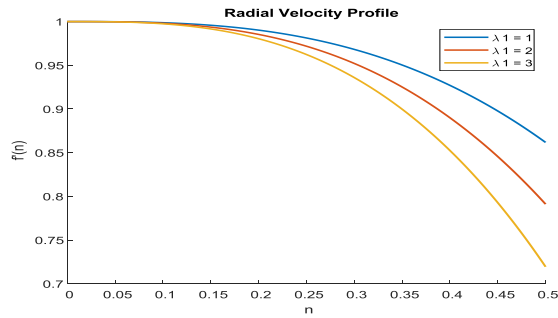


Fig. 6. Fig. 7.

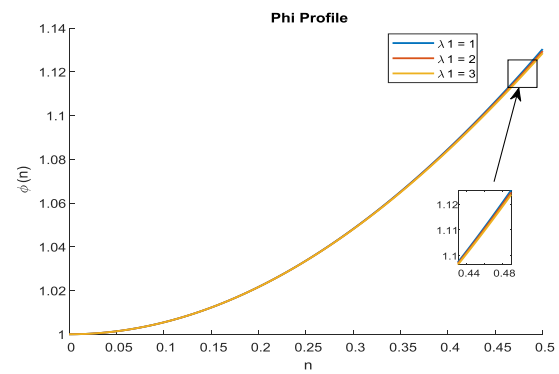
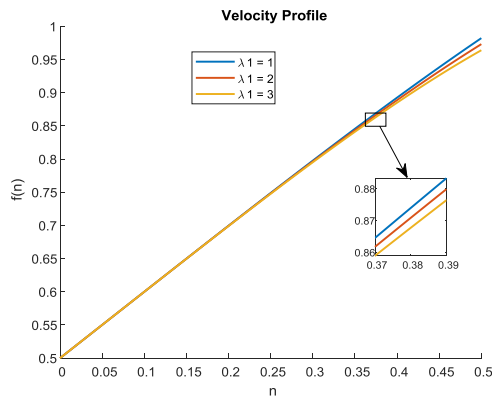


Fig. 8. Fig. 9.

Table 1:

| Nt | Nb | | |
|-------|----------|----------|----------|
| | 0.1 | 0.5 | 0.7 |
| f | 0.982159 | 0.982159 | 0.982159 |
| f' | 0.861721 | 0.861721 | 0.861721 |
| theta | 1.064059 | 1.044462 | 1.038563 |
| phi | 1.130395 | 1.130395 | 1.130395 |

Table 2:

| Pr | Nb | | |
|-------|------------|------------|------------|
| | 8.5 | 9 | 9.5 |
| f | 0.98215934 | 0.98215934 | 0.98215934 |
| f' | 0.86172091 | 0.86172091 | 0.86172091 |
| theta | 1.06405861 | 1.06405861 | 1.06405861 |
| phi | 1.54922818 | 1.58363407 | 1.61836176 |

Table 3:

| | Nb | | |
|-------|----------|----------|----------|
| | 0.3 | 0.5 | 0.7 |
| f | 0.982159 | 0.982159 | 0.982159 |
| f' | 0.861721 | 0.861721 | 0.861721 |
| theta | 1.064059 | 1.064059 | 1.064059 |
| phi | 1.079477 | 1.130395 | 1.179742 |

Table 4:

| | lambda 1 | | |
|-------|------------|------------|------------|
| | 1 | 2 | 3 |
| f | 0.98215934 | 0.97309733 | 0.96393957 |
| f' | 0.86172091 | 0.79107266 | 0.71940049 |
| theta | 1.06405861 | 1.06350254 | 1.0629419 |
| phi | 1.13039496 | 1.12945651 | 1.12851052 |

No conflict of Interest

References

- [1] Abel, M. S., Mahesha, N., &Tawade, J. (2009). Heat transfer in a liquid film over an unsteady stretching surface with viscous dissipation in presence of external magnetic field. *Applied Mathematical Modelling*, 33(9), 3430-3441. <https://doi.org/10.1016/j.apm.2008.11.021>
- [2] Abel, M. S., & Mahesha, N. (2008). Heat transfer in MHD viscoelastic fluid flow over a stretching sheet with variable thermal conductivity, non-uniform heat source, and radiation. *Applied Mathematical Modelling*, 32(10), 1965-1983.
- [3] Agarwalla, S., & Ahmed, N. (2017). MHD mass transfer flow past an inclined plate with variable temperature and plate velocity embedded in a porous medium. *Heat Transfer-Asian Research*, 47(1), 27-41. <https://doi.org/10.1002/htj.21288>
- [4] Choi, S. U. S., & Eastman, J. A. (1995, November 12-17). Enhancing thermal conductivity of fluids with nanoparticles. *ASME International Mechanical Engineering Congress & Exposition*, San Francisco, CA.
- [5] Cramer, K. R., & Pai, S. I. (1973). *Magnetofluid dynamics for engineers and applied physicists*. McGraw-Hill.
- [6] Das, S. (2016). An analytical study of the unsteady mixed convection flow of the Jeffrey fluid over an oscillating vertical plate with thermal radiation effects and chemical reaction. *Alexandria Engineering Journal*, 55(2), 1039-1058
- [7] Hayat, T., & Mustafa, M. (2010). Influence of thermal radiation on the unsteady mixed convection flow of a Jeffrey fluid over a stretching sheet. *Zeitschrift Für Naturforschung A*, 65(8-9), 711-719. <https://doi.org/10.1515/zna-2010-8-913>
- [8] Hayat, T., Abbas, Z., Pop, I., & Asghar, S. (2010). Effects of radiation and magnetic field on the mixed convection stagnation-point flow over a vertical stretching sheet in a porous medium. *International Journal of Heat and Mass Transfer*, 53(1-3), 466-474. <https://doi.org/10.1016/j.ijheatmasstransfer.2009.09.010>
- [9] Hayat, T., Waqas, M., Shehzad, S. A., & Alsaedi, A. (2015). MHD stagnation point flow of Jeffrey fluid by a radially stretching surface with viscous dissipation and Joule heating. *Journal of Hydrology and Hydromechanics*, 63(4), 311-317. <https://doi.org/10.1515/johh-2015-0038>
- [10] Noor, A., Nazar, R., Jafar, K., & Pop, I. (2014). Boundary-layer flow and heattransfer of nanofluids over a permeable moving surface in the presence of a coflowing fluid. *Advances in Mechanical Engineering*, 6, 521236. <https://doi.org/10.1155/2014/521236>
- [11] Nadeem, S., & Lee, C. (2012). Boundary layer flow of nanofluid over an exponentially stretching surface. *Nanoscale Research Letters*, 7(1), 94. <https://doi.org/10.1186/1556-276X-7-94>
- [12] Abd-Alla, A. M., Thabet, E. N., &Bayones, F. S. (2022). Numerical solution for MHD peristaltic transport in an inclined nanofluid symmetric channel with porous medium. *Scientific Reports*, 12(1), 3348. <https://doi.org/10.1038/s41598-022-07193-5>
- [13] Srikant G V P N et al. (2014) "Heat and mass transfer with MHD nanofluid with chemical reaction effects", *International journal of mechanical and production engineering*, vol2, issue 3.
- [14] Achala. L. N and Sathyanarayana. S. B, (2011) "Fluid over nonlinearly stretching sheet with magnetic field by homotopy analysis method ", *JI of Applied Mathematics and fluid mechanics*, vol.3, No. 1,15-22
- [15] Krishnendu Bhattacharyya (2013) "Boundary layer stagnation-point flow of Casson fluid and heat transfer towards a stretching/shrinking sheet", *Frontiers in heat and mass transfer (FHMT)*, vol4, 023003
- [16] M. Qasim (2013) "Heat and mass transfer in a Jeffrey fluid over a stretching sheet with heat source/sink", *Alexandria engineering journal*, vol52, 571-575
- [17] Masarath Jabeen*, V Dhanalaxmi, Transfer of heat and mass of a Jeffrey Fluid over a linearly stretching sheet with chemical reaction: Numerical study
- [18] Masarath Jabeen*, V Dhanalaxmi, Combined effect of viscous Dissipation and Ohmic heating on MHD Jeffrey nanofluid flow with magnetic dipole effect
- [19] Masarath Jabeen*, V Dhanalaxmi, Transfer of heat of a Jeffrey Fluid over a linearly stretching sheet with chemical reaction: Numerical study

- [20] Mohammed. J. Uddin et al. (2012) "MHD free convective boundary layer flow of a nanofluid past a flat vertical plate with Newtonian heating boundary condition", PLOS ONE 7(11) E49499 doi:10.1371/journal.pone.0049499
- [21] Sushma V Jakati¹, Raju B T², Achala L Nargund³, S B Sathyanarayana⁴, The Effect of Brownian motion and Soret effect on nanofluids stretching for Jeffrey fluid model
- [22] Ghafouri et al. (2017) "Effect of variable thermal conductivity models on the combined convection heat transfer in a square enclosure filled with water-alumina nanofluid", journal of applied mechanics and technical physics, vol58, no 1.103-115
- [23] Bhattacharyya K, Layek G. Magnetohydrodynamic boundary layer flow of nanofluid over an exponentially stretching permeable sheet. Physics research international. 2014;2014
- [24] Hayat T, Aziz A, Muhammad T, Alsaedi A. Three-dimensional flow of nanofluid with heat and mass flux boundary conditions. Chinese Journal of Physics. 2017;55:1495-510
- [25] Sulochana C, Ashwinkumar G, Sandeep N. Similarity solution of 3D Casson nanofluid flow over a stretching sheet with convective boundary conditions. Journal of the Nigerian Mathematical Society. 2016;35:128-41.
- [26] Rana S, Mehmood R, Akbar NS. Mixed convective oblique flow of a Casson fluid with partial slip, internal heating and homogeneous–heterogeneous reactions. Journal of Molecular liquids. 2016;222:1010-9.
- [27] Zaib A, Bhattacharyya K, Uddin M, Shafie S. Dual solutions of non-Newtonian Casson fluid flow and heat transfer over an exponentially permeable shrinking sheet with viscous dissipation. Modelling and Simulation in Engineering. 2016;2016.
- [28] Vajravelu K, Prasad K, Datti P, Raju B. Convective flow, heat and mass transfer of Ostwald-de Waele fluid over a vertical stretching sheet. Journal of King Saud University-Engineering Sciences. 2017;29:57-67.
- [29] Turkyilmazoglu M. Multiple solutions of heat and mass transfer of MHD slip flow for the viscoelastic fluid over a stretching sheet. International Journal of Thermal Sciences. 2011;50:2264-76.
- [30] Sahoo B, Poncet S. Flow and heat transfer of a third grade fluid past an exponentially stretching sheet with partial slip boundary condition. International Journal of Heat and Mass Transfer. 2011;54:5010-9.